ELSEVIER

Journal of Organometallic Chemistry 562 (1998) 53–60

Journal of Organo metallic Chemistry

Preparation and characterization of $(R_2N)_2VCl_2$ [R = Cy, i-Pr] and its activity as olefin polymerization catalyst[1]

Natalie Desmangles [a], Sandro Gambarotta [a,*], Corinne Bensimon [a], Stephen Davis [b], Hayder Zahalka [b]

[a] *Department of Chemistry, University of Ottawa, Ottawa, Ontario K1N 6N5, Canada*
[b] *Department of Research and Development, Bayer Incorporated, Sarnia, Ontario, Canada*

Received 27 June 1997

Abstract

Reaction of $VCl_3(THF)_3$ with one equivalent of R_2NLi [R = i-Pr, Cy] formed the tetravalent $(R_2N)_2VCl_2$ [R = i-Pr (**1a**), Cy (**1b**)] which was isolated in crystalline form. The formation of these species is likely to be ascribed to a disproportionation reaction since a divalent vanadium complex, $VCl_2(TMEDA)_2$ complex was isolated upon treatment of the reaction mixtures with TMEDA. Complexes **1** can be alkylated with RLi to yield the corresponding $(R_2N)_2VR_2$ (**2**) derivatives in good yield. Preliminary data on ethylene–propylene (EP) co-polymerization obtained with compounds **1** in conjunction with various aluminum alkyl compounds are described. © 1998 Elsevier Science S.A. All rights reserved.

Keywords: Vanadium; Alkylamido; Alkyl; Ethylene–propylene co-polymerization

1. Introduction

The employment of group 4 metals and lanthanides plays a primary role in the vast literature of Ziegler–Natta catalysis [1]. This is mainly due to the distinct versatility of the metallocenic derivatives of these metals for which a wealth of synthetic methodologies were developed [2]. By contrast, limited information is available for the group 5 elements in spite of the fact that a few medium and high valent vanadium complexes [VCl_4, $VOCl_3$ and $V(acac)_3$] display, in conjunction with organoaluminum co-catalyst, a remarkable catalytic activity as Ziegler–Natta polymerization catalysts [3]. These species are currently used for the commercial production of ethylene–propylene–diene elastomers [EP(D)M] ([3]s). Vanadium compounds, although exhibiting lower catalytic activity than group 4 metal metallocene, display the advantage to perform well in a variety of oxidation states by producing polymers and copolymers with desirable physical properties and a high level of tacticity [4]. In contrast to this great potential, vanadium was largely ignored by the recent revival of interest for the new generation of Ziegler–Natta catalysts since the focus of the current polyolefins literature mainly remains on the employment of group 4 metals with a minor emphasis on lanthanides. Conversely, developing new vanadium-based Ziegler–Natta type catalysts may pose significant synthetic challenges given that group 5 metallocene or cyclopentadienyl derivatives do not show a particularly strong inclination towards insertion reactions [5] (an obvious prerequisite for Ziegler–Natta catalysis). Thus in an attempt to take advantage of the potential of vanadium as a Ziegler–Natta catalyst, we have recently embarked on a project aimed to the development of new vanadium complexes containing anionic organic amides as ancillary ligands [6]. What is making this

---

* Corresponding author. Tel.: +1 613 5625199; fax: +1 613 5625170.

[1] Dedicated to Prof. R. Bruce King on the occasion of his 60th birthday.

0022-328X/98/$19.00 © 1998 Elsevier Science S.A. All rights reserved.
PII S0022-328X(98)00366-0

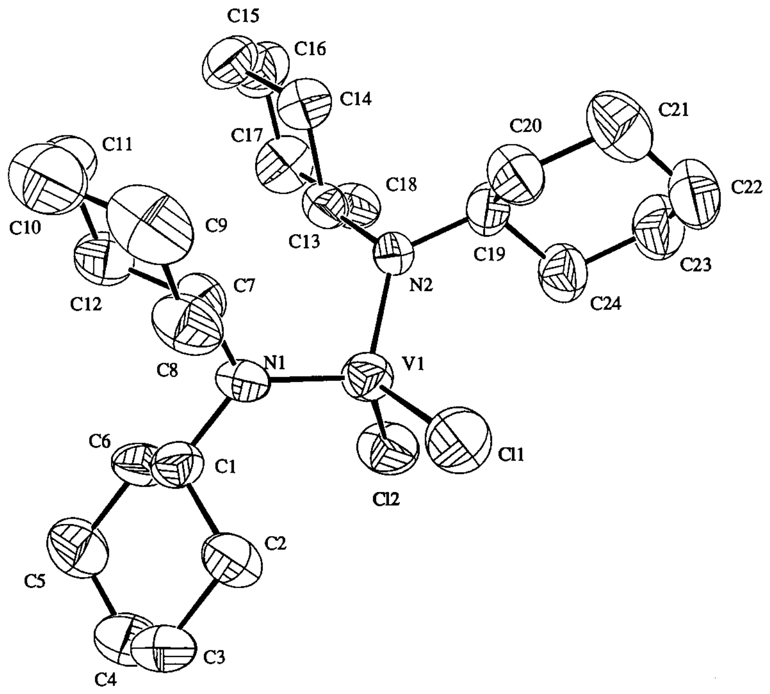

Fig. 1. Thermal ellipsoid plot of **1b**. Thermal ellipsoids are drawn at the 50% probability level.

family of ligands particularly attractive is the possibility of fine tuning the electronic and steric features around the metal center through a virtually unlimited choice of the organic substituents attached to the nitrogen donor atom.

We describe in this paper the preparation of novel V(IV) amide complexes as well as a preliminary study of their organometallic chemistry and utility for olefin polymerization.

2. Results and discussion

We have recently described the reaction of $VCl_3(THF)_3$ with anionic organic amides forming a series of monomeric and dimeric bis-amide V(III) $(R_2N)_2VCl$ derivatives [7]. The fact that these complexes can be prepared in a rather straightforward manner via chlorine replacement reaction, implies that a mononuclear '(amide)VCl_2' complex is formed as a transient intermediate. In an attempt to isolate and characterize this intermediate species we have reacted $VCl_3(THF)_3$ with one equivalent of R_2NLi [R = i-Pr, Cy, Bz]. The reaction proceeds forming an intense red color upon mixing. Dark orange crystals of $(R_2N)_2VCl_2$ [R = i-Pr (**1a**), Cy (**1b**)] were isolated after suitable work-up upon cooling their hexane solutions. The complexes are paramagnetic, moderately air sensitive and test positive for the presence of chlorine and negative for lithium. X-ray fluorescence experiments yielded a 1:2 vanadium to chlorine ratio. Combustion analysis data were consistent with the proposed formulation while the magnetic moments, calculated on the basis of this formula, were always in agreement for the d^1 electronic configuration of tetravalent vanadium.

The molecular connectivity and the formula were confirmed by a crystal structure obtained in the case of the cyclohexyl derivative **1b**. The complex is monomeric and is formed by a vanadium atom surrounded by two amide groups and two chlorine atoms which impose a distorted tetrahedral coordination geometry to the metal center [N1–V1–Cl1 = 105.0(2), N1–V1–N2 = 106.8(2), N1–V1–Cl2 = 113.6(2), N2–V1–Cl2 = 104.0(2), N2–V1–Cl1 = 114.2(2)°] (Fig. 1). The V–Cl distances [V1–Cl1 = 2.256(2), V1–Cl2 = 2.217(2) Å] and angles [Cl1–V1–Cl2 = 113.3(1)°] fall in the expected range. As usual, the coordination geometry around the amide nitrogen is trigonal planar [V1–N1–C1 = 124.8(4), V1–N1–C7 = 120.1(4)°] which, together with the short V–N distances [V1–N1 = 1.808(5), V1–N2 = 1.834(5)Å], suggests the presence of a significant extent of V=N double bond.

The formation of a tetravalent vanadium from a trivalent starting material is rather surprising given that anionic organic amides are well known to act as reducing agents [8] and to be able to stabilize low-valent states [9]. Therefore, the formation of these species has to be explained with the occurrence of a disproportionation, perhaps similar to that observed in the case of dinuclear Zr(III) derivatives [10]. In this event, a V(II) species [probably $VCl_2(THF)_x$] should be formed as byproduct of the reaction. To probe this possibility, we

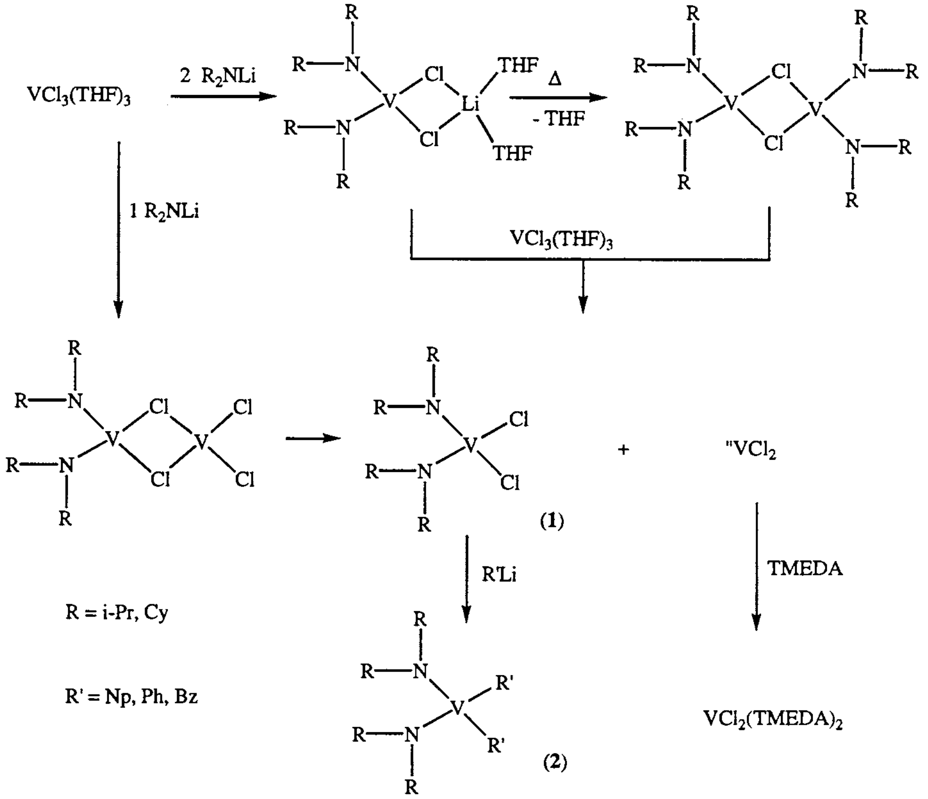

Scheme 1. Reaction scheme depicting production of complexes **1** and **2**.

have treated the reaction mixture with TMEDA. The treatment produces a light blue crystalline solid in low yet significant yield which was identified as $VCl_2(TMEDA)_2$ by comparison of the spectroscopic properties with those of an analytically pure sample.

The most simple manner to envision the process and to account for these observations is through the reaction sequence depicted in Scheme 1.

The reaction may be explained by assuming the formation of an asymmetric and dinuclear intermediate which undergoes slow and spontaneous cleavage to originate the two V(IV) and V(II) moieties. The stability of the two species is likely to be the thermodynamic driving force for the cleavage of the dinuclear structure. In agreement with this hypothesis, the reaction of both $[(R_2N)_2V(\mu\text{-Cl})]_2$ and $(R_2N)_2V(\mu\text{-Cl})_2Li(THF)_2$ with VCl_3 also gave similar yield of $(R_2N)_2VCl_2$. As for above, even in this case 'VCl_2' was isolated and identified as $VCl_2(TMEDA)_2$ after treating the reaction mixture with TMEDA.

Attempts to replace the chlorine atoms in **1** with alkyls functions were carried out with a few alkyl lithium reagents. The reactions of **1** and RLi proceeded rapidly at − 10°C in ether or hexane to produce the corresponding dialkyl derivatives $(R_2N)_2VR_2$ [R = Np (**2a**), Ph (**2b**), Bz (**2c**)]. All these compounds were isolated in crystalline form as dark brown air sensitive materials. All the compounds tested negative for chlorine, thus confirming that both the chlorine atoms were replaced and satisfactory combustion analysis data in agreement with the proposed formulation were obtained for all the compounds. The magnetic moments were in all cases in agreement with the d^1 electronic configuration expected for a V(IV) species. Compounds **2** are only moderately stable at room temperature (r.t.) and rapidly decompose at about 60°C to form new species whose structure is currently under investiga-tion.

In the case of the neopentyl derivative, the molecular connectivity was elucidated by an X-ray crystal structure. The structure consists of a distorted tetrahedral vanadium center [N1–V1–N2 = 117.5(1), N1–V1–C25 = 110.1(1), N1–V1–C30 = 106.0(1), N2–V1–C25 = 105.6(1), N2–V1–C30 = 111.3(1), C25–V1–C30 = 105.8(1)°] surrounded by two nitrogen atoms of the two amides and two alkyl groups (Fig. 2). The V–N distances are normal [V1–N1 = 1.877(2), V1–N2 = 1.878(2) Å] and compare well with those of the dichloro derivative **1b**. The V–C distances are also in the expected range [V1–C25 = 2.088(3), V1–C30 = 2.095(3) Å]. The coordination geometry around the nitrogen atom is trigonal planar as expected [V1–N1–C1 = 127.1(2), V1–N1–C7 = 115.9(2), C1–N1–C7 = 116.9(2)°].

Not surprisingly, complexes **2** did not display any significant olefin polymerization activity under the usual reaction conditions. Just a violent reaction was

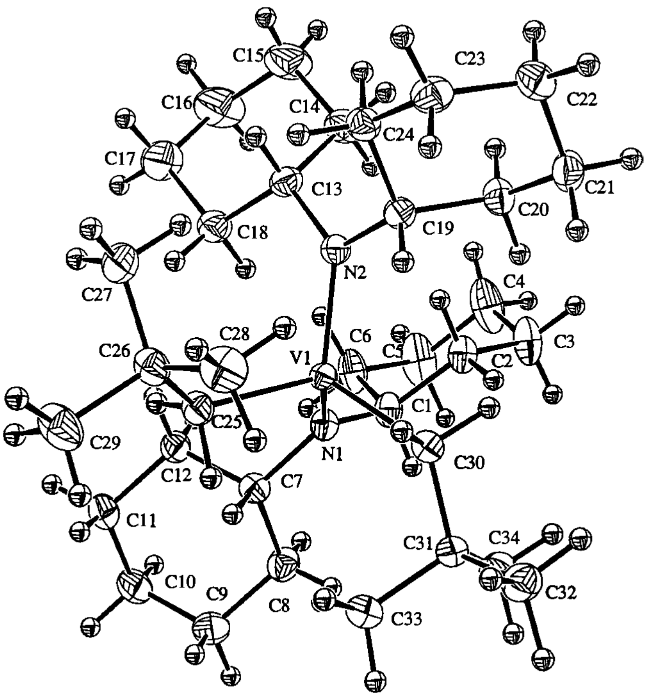

Fig. 2. Thermal ellipsoid plot of **2a**. Thermal ellipsoids are drawn at the 50% probability level.

observed with butadiene leading to the formation of a viscous polymer. Even attempts to improve reactivity by treatment with Lewis acids such as VCl_3 or $(F_5C_6)_3B$ did not modify the inertness of this system toward polymerization. Conversely, simple treatment of **2** with anhydrous $AlCl_3$ gave an active polymerization catalyst (188 Kg of polyethylene (PE) mol^{-1} catalyst h^{-1} at a maximum pressure of 1 bar). These results clearly show that the concomitant presence of both vanadium and aluminium is indeed necessary to produce catalytic activity. Accordingly, complexes **1** act as ethylene polymerization catalysts at r.t. and under one atmosphere of ethylene while in conjunction with a wide variety of aluminum alkyl co-catalysts (Me_3Al, Et_3Al, $EtAlCl_2$, $Et_{1.5}AlCl_{1.5}$, i-$BuAlCl_2$). We have observed that upon mixing the catalyst with the co-catalyst an immediate color change occurred in the hexane solution thus suggesting that the coordination sphere of the vanadium atom was modified by the interaction with the aluminium co-catalyst. Unfortunately, attempts to isolate and characterize the catalytically active species led to highly pyrophoric microcrystalline catalysts in good yield, whereas efforts to grow crystals of suitable size for crystal structure determination were so far unsuccessful.

By using the most effective catalyst/co-catalyst system, the production of PE reached the amount of about 265 Kg of polymer mol^{-1} catalyst h^{-1} at 1 bar. After the initial production of ethylene during the first 15–30 min, the reaction proceeded at low steady rate for about 20 h when no significant production of PE was observed anymore. This indicates that the catalyst was probably deactivated. Addition of chlorinated hydrocarbon (BzCl, $ClCH_2CH_2Cl$ or $CHCl_3$) to the reaction mixture, followed by addition of the co-catalyst, restarted the polymerization. The deactivation of vanadium Ziegler–Natta catalysts is commonly ascribed to the reduction of the metal center (probably through β-H elimination) towards formation of divalent species [3]. However, homopolymerization of ethylene with trivalent $(R_2N)_2V(\mu\text{-}Cl)_2Li(THF)_2$ or $[(R_2N)_2V(\mu\text{-}Cl)]_2$ [7] did not give any appreciable polymerization reaction, while treatment of these complexes with halogenated hydrocarbons formed the tetravalent $(R_2N)_2VCl_2$ catalyst. On the basis of these observations, we tentatively suggest that the catalyst deactivation in our system is probably caused by the reduction of $(R_2N)_2VCl_2$ to the corresponding trivalent species.

Complexes **1** were tested for ethylene–propylene (EP) co-polymerization activity with a series of $AlR_xCl_{(3-x)}$ under 2 bar pressure. The results are shown in Table 1. Under the conditions employed, activity was negligible with Et_3Al but increased with increasing chlorine content. The activity reached a maximum with Et_2AlCl_3 which makes this species a promising catalyst for the production of elastomers. The FTIR spectrum (Fig. 3) is typical of a random copolymer as evidenced by the fingerprint region from 700 to 1200 cm^{-1}. The ethylene content, evaluated via IR spectroscopy by using the ratio of peak heights of the two resonances at 1155 and 720 cm^{-1} after calibration with known standards ac-

Table 1
Ethylene–propylene co-polymerization activity of complex **1**

Catalyst $(R_2N)_2VCl_2$	Co-catalyst	Activity (kg EP mol^{-1} V h^{-1})	Composition (wt% ethylene)
R = i-Pr	Et3Al	24	—
	Et2AlCl	80	—
	Et1.5AlCl1.5	860	73
	EtAlCl2	330	71
R = Cy	Et3Al	40	—
	Et2AlCl	135	73
	Et1.5AlCl1.5	330	73
	EtAlCl2	140	—

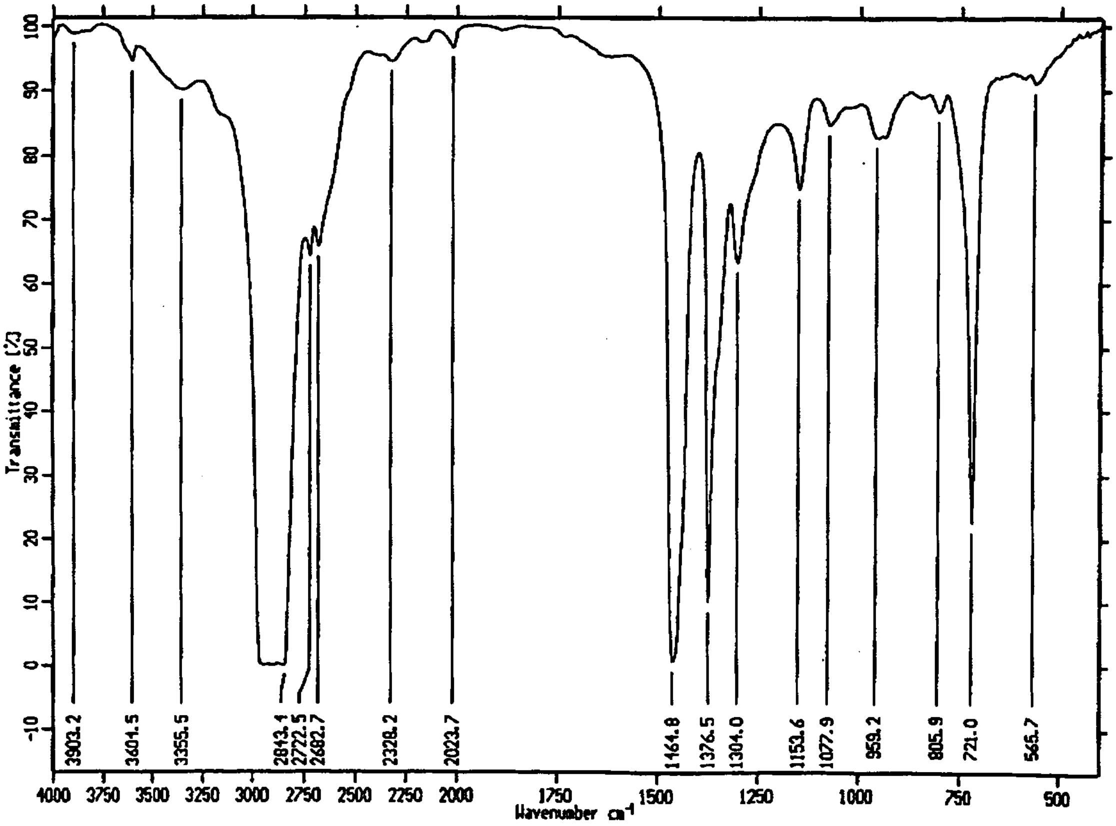

Fig. 3. FTIR of the EP copolymer.

cording to ASTM procedure D-3900, was typically in the range 71–73%. In a typical experiment carried out on (i-$Pr_2N)_2VCl_2$ and aluminum sesquichloride as a co-catalyst, the molecular weight was significantly high (Mw = 2293000, Mw/Mn = 3.0).

3. Experimental section

All operations were performed under inert atmosphere by using standard Schlenk techniques. Cy_2NLi [11] and (i-Pr)$_2$NLi [12] were prepared according to published procedures. Alkyl lithium derivatives were prepared according to standard procedures. Ethylene, propylene (Matheson) were dried over a column of molecular sieves. Aluminum alkyls solutions in hexane (Aldrich) were used as received. IR spectra were recorded on a Mattson 9000 FTIR instrument from Nujol mulls prepared in a dry-box. Samples for magnetic susceptibility measurements were weighed inside a dry-box equipped with an analytical balance, and sealed into calibrated tubes. Magnetic measurements were carried out with a Gouy balance (Johnson Matthey) at r.t. The magnetic moments were calculated following standard methods [13] and corrections for underlying diamagnetism were applied to data [14]. Elemental analyses were carried out with a Perkin Elmer 2400 CHN analyzer. Ratios between heavy atoms were determined by X-ray fluorescence by using a Philips 2400 instrument.

Evaluation of the catalysts were carried out using ethylene–propylene co-polymerization in hexane solution at 2 bar total pressure and 22°C. Polymerization were carried out in 200 ml of hexane in magnetically agitated glass reactors at 2 bar pressure using a continuous flow of 1000 sccm of both ethylene and propylene. After equilibration of the hexane with the EP feed at 22°C, 0.2 mmol of co-catalyst were added followed by the addition of 5 μmol vanadium catalyst. These conditions gave a final concentration of 25 μM [catalyst] and 40/1 Al/V. Polymerization was carried out for 15 min followed by addition of 2 ml ethanol and depressurization. The EP rubber was recovered by solvent evaporation.

3.1. Synthesis of *(i-$Pr_2N)_2VCl_2$ (1a)*

A suspension of $VCl_3(THF)_3$ (1.07 g, 2.8 mmol) in THF (75 ml) was treated at r.t. with freshly prepared i-Pr_2NLi (0.33 g, 3.0 mmol). The color immediately turned dark red. After stirring overnight at r.t., the solvent was evaporated in vacuo. The residual oil was redissolved in hexane (100 ml) and the resulting suspension filtered, concentrated to small volume and allowed to stand at − 78°C. Dark red crystals of $(i\text{-}Pr_2N)_2VCl_2$ (0.33 g, 1.0 mmol, 71% based on Liamide) separated. IR (Nujol mull, cm^{-1}) ν: 2897(br), 2687(br), 1457(s), 1372(s), 1338(m), 1261(w), 1185(w), 1145(m), 1124(m), 1101(s), 970(w), 924(w), 859(w), 814(w), 780(w), 723(w). Anal. Calc. (found) for $C_{12}H_{28}N_2Cl_2V$: C 44.73 (44.70), H 8.76 (8.72), N 8.69 (9.10). $\mu_{eff} = 1.89\ \mu_B$.

3.2. Synthesis of *$(Cy_2N)_2VCl_2$ (1b)*

3.2.1. Method A

Freshly prepared Cy_2NLi (0.47 g, 2.83 mmol) was added to a red suspension of $VCl_3(THF)_3$ (1.05 g, 2.81 mmol) in THF (75 ml) at r.t. The color immediately turned dark red and the resulting solution was stirred overnight at r.t. After evaporation of the solvent to dryness, hexane (100 ml) was added to the oily residue. The resulting suspension was filtered and the solution was concentrated to small volume. Dark red crystals of $(Cy_2N)_2VCl_2$ (0.57 g, 1.2 mmol, 42%) were separated after allowing the red solution to stand at − 30°C for two days. IR (Nujol mull, cm^{-1}) ν: 2907(br), 2690(w), 1455(s), 1376(s), 1342(m), 1258(w), 1145(vw), 1136(m), 1077(m), 1026(m), 954(m), 889(m), 842(m), 804(m), 784(w), 723(w). Anal. Calc. (found) for $C_{24}H_{44}N_2Cl_2V$: C 59.75 (60.41), H 9.19 (9.50), N 5.81 (6.02). $\mu_{eff} = 2.00\ \mu_B$.

3.2.2. Method B

Brown solid $[(Cy_2N)_2VCl]_2$ (1.7 g, 1.9 mmol) was added to a red suspension of $VCl_3(THF)_3$ (1.46 g, 3.9 mmol) in THF (100 ml) at r.t. The color turned instantaneously dark red. After evaporation of the solvent in vacuo, the dark red oil was dissolved in hexane (75 ml). Dark red crystals of **1b** (1.7 g, 3.6 mmol, 90% based on $VCl_3(THF)_3$) were obtained after allowing the red solution to stand at − 30°C overnight.

3.2.3. Method C

Solid Cy_2NLi (4.45 g, 23.7 mmol) was added to a suspension of $VCl_4(dme)$ (3.3 g, 11.8 mmol) in THF (100 ml) at − 78°C. The color gradually changed to the purple brown and after 8 h stirring at r.t., the solvent was removed in vacuo. The residue was extracted with hexane and filtered to remove LiCl. The filtrate was allowed to stand at − 30°C overnight yielding dark brown crystals of **1b** (3.1 g, 6.4 mmol, 55%). The compound was identified by comparison of the analytical and spectroscopic data of an analytically pure sample.

3.3. Isolation of *$VCl_2(TMEDA)_2$*

3.3.1. Method A

Solid Cy_2NLi (0.95 g, 5.7 mmol) was added to a red suspension of $VCl_3(THF)_3$ (1.78 g, 4.76 mmol) in THF (75 ml) at r.t. The color turned dark red. After stirring for 30 min, the addition of TMEDA (1.45 ml, 9.61 mmol) to the dark red solution did not cause any significant color change. After evaporation of the solvent to dryness, hexane (75ml) was added to the dark residue. The addition of hexane caused the precipitation of a light blue solid mixed with a light brown solid. After filtration the mixed solid was recrystallized from THF affording analytically pure light blue crystals of $VCl_2(TMEDA)_2$ (35%) which were identified by comparison of the spectroscopic data with those of an analytically pure sample.

3.3.2. Method B

Freshly distilled TMEDA (0.82 ml, 5.3 mmol) was added to a red suspension of $VCl_3(THF)_3$ (1.00 g, 2.7 mmol) in THF (75 ml) at r.t. Addition of solid Cy_2NLi (0.51 g, 3.0 mmol) to the resulting violet solution turned the color light brown. After evaporation of the solvent in vacuo, the addition of diethyl ether (75 ml) caused the precipitation of a light blue microcrystalline $VCl_2(TMEDA)_2$ (0.71g, 2.0 mmol, 74%) which was identified by comparison of the spectroscopic data with those of an analytically pure sample.

3.4. Synthesis of *$(Cy_2N)_2VNp_2 \cdot 0.25$hexane (2a)*

Solid NpLi (0.33 g, 4.22 mmol) was added to a dark red solution of $(Cy_2N)_2VCl_2$ (0.98 g, 2.0 mmol) in hexane (75 ml) at r.t. The color slightly turned dark orange and the resulting solution was stirred overnight at r.t. After filtration of LiCl, the solution was concentrated to 20–30 ml and allowed to cool down to − 30°C overnight. Dark crystals of $(Cy_2N)_2VNp_2$ (0.23 g, 0.46 mmol, 23%) were separated. IR (Nujol mull, cm^{-1}) ν: 2905(s), 2689(w), 1456(s), 1375(sh), 1230(w), 1093(m), 1026(m), 956(sh), 891(w), 843(m), 802(m), 722(sh). Anal. Calc. (found) for $C_{34}H_{66}N_2V \cdot 0.25$hexane: C 73.90 (73.56), H 12.23 (12.01), N 4.92 (4.66). $\mu_{eff} = 1.85\ \mu$B.

3.5. Synthesis of *$(Cy_2N)_2VPh_2$ (2b)*

Solid PhLi (0.29 g, 3.45 mmol) was added to a dark red solution of $(Cy_2N)_2VCl_2$ (0.66 g, 1.37 mmol) in hexane (75 ml) at r.t. The color slightly turned dark orange and the resulting solution was stirred overnight at r.t. After filtration of LiCl, the solution was concentrated to about 25 ml and allowed to stand at − 30°C overnight. Dark microcrystalline solid of $(Cy_2N)_2VPh_2$ (0.58 g, 1.0 mmol, 73%) were separated. IR (Nujol mull, cm^{-1}) ν: 2907(br), 2692(w), 1457(s), 1447(vw), 1376(sh), 1366 (vw), 1260(m), 1100(vw), 1090(vw), 1080(vw), 1070(m), 1059(vw), 1038(m), 960(shw), 891(w), 813(vw), 803(m), 722(sh), 698(sh). Anal. Calc. (found) for $C_{36}H_{54}N_2V$: C 76.42 (76.11), H 9.62 (9.38), N 4.95 (4.88). $\mu_{eff} = 1.80\ \mu$B.

3.6. Synthesis of $(Cy_2N)_2VBz_2$ (2c)

A solution of BzMgCl (5.8 ml, 5.8 mmol, 1 M in ether) was added to a dark red solution of $(Cy_2N)_2VCl_2$ (1.4 g, 2.9 mmol) in hexane (75 ml) at r.t. The color turned brownish orange and the resulting solution was stirred overnight at r.t. After filtration of LiCl, the solution was concentrated to 20–30 ml and allowed to stand at −30°C overnight. Dark microcrystalline solid of $(Cy_2N)_2VBz_2$ (0.9 g, 1.5 mmol, 52%) were separated. IR (Nujol mull, cm^{-1}) ν: Anal. Calc. (found) for $C_{38}H_{58}N_2V$: C 76.86 (76.66), H 9.85 (9.69), N 4.72 (4.61). $\mu_{eff} = 1.77\ \mu B$.

3.7. X-ray crystallography

Data were collected at −153°C for suitable air-sensitive crystals mounted on a glass fiber inside a drybox and transferred under the liquid nitrogen stream of the cooling system of either Nonius CAD-4 or Siemens CCD X-ray diffractometers. The $\omega - 2\theta$ scan technique was used. Data were collected until 100° of 2θ for **1b** (Cu radiation) and to 57.0° for **2a** (Mo radiation). Cell constants and orientation matrices were obtained from the least-squares refinement of 25 centered reflections. The intensities of three standard reflections, measured after every 150 reflections, showed no statistically significant decay over the duration of the data collections. Data were corrected for Lorentz and polarization effects and for absorption (PSI scan). The structures were solved by direct methods resulting in locating all the non-hydrogen atoms. Their positions were refined anisotropically. Hydrogen atom positions were calculated but not refined. Complex **1b** contains two crystallographically-independent and nearly identical molecules in the lattice while complex **2a** has one disordered molecule of hexane per unit cell. Attempts to model the disorder did not improve the thermal parameters and the quality of the refinement. The data were processed using the NRCVAX software packages on a Silicon Graphics workstation. Refinements were carried out by using full-matrix least-squares techniques on F minimizing the function $\Sigma w(|F_0| - |F_c|)^2$, where $w = 4F_0^2/\sigma^2(F_0^2)$ and F_0 and F_c are the observed and calculated structure factors, respectively. Atomic scattering factors and anomalous dispersion terms were taken from the usual sources (Cromer and Waber) [15]. Details on the data collections and structure refinement are listed in Table 2. The final atomic coordinates are given as Supplementary Material (see below). Selected bond distances and angles are given in Table 3.

Table 2
Crystal data and structure analysis results

	1b	2a
Formula	$C_{24}H_{44}N_2VCl_2$	$C_{34}H_{66}N_2V \cdot 0.25C_6H_{14}$
Formula weight	482.48	575.39
Space group	*Pbna*	$P2_1/a$
a (Å)	15.669(4)	17.7491(2)
b (Å)	36.004(1)	10.6826(2)
c (Å)	18.871(4)	20.8487(3)
β (°)		109.479(1)_
V (Å^3)	10 646(4)	33726.8(1)
Z	8	4
Radiation (K_α Å)	1.54056	0.70930
T (°C)	−153	−153
D_{calc} (g cm^{-3})	1.205	1.026
μ_{calc} (cm^{-1})	50.4	2.9
R	0.048	0.053
R_w	0.051	0.77
GOF	2.02	1.91

$R = \Sigma\|F_0| - |F_c\|/\Sigma|F_0|$ and $R_w = [(\Sigma(|F_0| - |F_c|)^2/\Sigma w F_0^2)]^{0.5}$

Table 3
Selected bond distances (Å) and angles (°)

1b		2a	
V1–Cl1	2.226(2)	V1–N1	1.877(2)
V1–Cl2	2.217(2)	V1–N2	1.878(2)
V1–N1	1.808(5)	V1–C25	2.088(3)
V1–N2	1.834(5)	V1–C30	2.095(3)
Cl1–V1–Cl2	113.3(1)	C25–V1–C30	105.8(1)
Cl1–V1–N1	105.0(2)	N1–V1–N2	117.5(1)
Cl1–V1–N2	114.2(2)	N1–V1–C25	110.0(1)
Cl2–V1–N1	113.6(2)	N1–V1–C30	106.0(1)
Cl2–V1–N2	104.0(2)	N2–V1–C25	105.5(1)
V1–N1–C1	124.8(4)	N2–V1–C30	111.3(1)
V1–N1–C7	120.1(4)	C1–N1–C7	116.9(2)
V1–N1–C1	127.1(2)		
V1–N1–C7	115.8(2)		

4. Supplementary material available

Listing of atomic coordinates, thermal parameters, bond distances and angles for **1b** and **2a**.

Acknowledgements

This work was supported by the National Science and Engineering Council of Canada (NSERC operating grant) and by the generosity of Bayer (Sarnia, Ontario).

References

[1] See for example: (a) G. Natta, P. Pino, P. Corradine, F. Danusso, E. Mantica, G. Mazzanti, G. Moraglio, J. Am. Chem. Soc. 77 (1955) 1708. (b) K. Ziegler, Belgium Patent 553,362 91953). (c) P. Pino, R. Mulhaupt, Angew. Chem. Int. Ed. Engl.

19 (1980) 857 and ref. cited therein. (d) A.S. Guram, R.F. Jordan, in: E.W. Abel, F.G.A. Stone, G. Wilkinson (Eds.), Comprehensive Organometallic Chemistry, Pergamon, Oxford, 1995 and ref. cited therein.

[2] See for example: (a) R.F. Jordan, Adv. Organomet. Chem. 32 (1991) 325. (b) H.H. Brintzinger, D. Fisher, R. Mulhaupt, B. Rieger, R.M. Waymouth, Angew. Chem. Int. Ed. Engl. 34 (1995) 1143. (c) M. Bochmann, J. Chem. Soc. Dalton Trans. 255 (1996).

[3] (a) H. Sinn, W. Kaminski, in: F.G.A. Stone, R. West (Eds.), Advanced Organometallic Chemistry, Academic Press, New York, 1980. (b) Y. Doi, N. Tokuhiro, M. Nunomura, H. Miyake, S. Suuki, K. Soga, in: W. Kaminsky, H. Sinn (Eds.), Transition Metals and Organometallics as Catalysts for Olefin Polymerization, Springer-Verlag, Berlin, 1988. (c) W.L. Carrick, J. Am. Chem. Soc. 80 (1958) 6455. (d) D.L. Christman, J. Polymer Sci. A-1, 1972, 471. (e) I.G. Pasquon, U. Giannini, in: J.R. Anderson, M. Boudart (Eds.), Catalysis, Springer-Verlag, Berlin, 1984. (f) W.L. Carrick, R.W. Kluiber, E.F. Bonner, L.H. Wartman, F.M. Rugg, J.J. Smith, J. Am. Chem. Soc. 82 (1960) 3883. (g) M.H. Lehr, Macromolecules 1 (1968) 178. (h) D.L. Christman, G.I. Keim, Macromolecules 1 (1968) 358. (i) E. von Junghanns, A. Gumboldt, G. Bier, Makromol. Chem. 101 (1967) 229. (j) M.H. Lehr, C.J. Carmen, Macromolecules 2 (1969) 217. (k) E.W. Duck, D. Grant, J.R. Horder, et al., Eur Polymer J. 10 (1974) 481. (l) V.J. Murphy, H. Turner, Organometallics 16 (1997) 2495. (m) S. Schuere, J. Fisher, J. Kress, Organometallics 14 (1995) 2627. (n) F.J. Feher, R.L. Blanski, J. Am. Chem. Soc. 114 (1992) 5886. (o) F.J. Feher, J.F. Walzer, R.L. Blanski, J. Am. Chem. Soc. 113 (1991) 3618. (p) F.J. Feher, R.L. Blanski, Organometallics 12 (1993) 958. (r) F.J. Feher, J.F. Walzer, Inorg. Chem. 30 (1991) 1689. (s) S.C. Davis, W. von Hellens, H. Zahalka, in: J.C. Salamone (Ed.), Polymer Material Encyclopedia, vol. 3, CRC Press, Boca Raton, FL, 1996. (t) S. Cucinella, A. Mazzei, US Patent 3,711,455, CI. 260-85.3, (1973).

[4] (a) J. Boor Jr., E.A. Youngman, J. Polymer Sci. A-1, 4 (1966) 1861. (b) A. Zambelli, G. Natta, I. Pasquon, J. Polymer Sci. C, 4 (1964) 411. (c) P. Pino, R. Mulhaupt, Angew. Chem. Int. Ed. Engl. 19 (1980) 857. (d) A. Zambelli, A. Proto, P. Longo, in: G. Fink, R. Mulhaupt, H.H. Brintzinger (Eds.), Ziegler Natta Catalysis, Springer-Verlag, Berlin, 1995.

[5] See for example: (a) D.F. Foust, R.D. Rogers, M.D. Rausch, J.L. Atwood, J. Am. Chem. Soc. 104 (1982) 5646. (b) V.C. Gibson, J.E. Bercaw, W.J. Bruton, R.D. Sanner, Organometallics 5 (1986) 976.

[6] (a) S.I. Song, P. Berno, S. Gambarotta, J. Am. Chem. Soc. 116 (1994) 6927. (b) N. Desmangles, H. Jenkins, K.B. Ruppa, S. Gambarotta, Can. J. Chem. (1996) 250. (c) P. Berno, R. Minhas, S. Hao, S. Gambarotta, Organometallics 13 (1994) 1052. (d) P. Berno, S. Gambarotta, Organometallics 13 (1994) 2569. (e) P. Berno, S. Gambarotta, Angew. Chem. Int. Ed. Engl. 34 (1995) 822. (f) J. Jubb, L. Scoles, H. Jenkins, S. Gambarotta, Chem. Eur. J. (1996) 767. (g) J.I. Song, S. Gambarotta, Chem. Eur. J. 2 (1996) 1258.

[7] P. Berno, M. Moore, R. Minhas, S. Gambarotta, Can. J. Chem. (in press).

[8] (a) M.H. Chisholm, F.A. Cotton, B.A. Frenz, W.W. Reichert, L.W. Shive, B.R. Stults, J. Am. Chem. Soc. 98 (1976) 4469. (b) M.H. Chisholm, W.W. Reichert, J. Am. Chem. Soc. 96 (1974) 1249. (c) D.C. Bradley, M.H. Chisholm, J. Chem. Soc. A (1971) 1511. (d) M.H. Chisholm, F.A. Cotton, B.A. Frenz, L.W. Shive, B.R. Stults, J. Chem. Soc. Chem. Comm. (1974) 480. (e) J.R. Dilworth, S.J. Harrison, R.A. Henderson, D.R.M. Walton, J. Chem. Soc. Chem. Commun. (1984) 176.

[9] (a) D.C. Bradley, M.B. Hursthouse, K.M.A. Malik, R. Moseler, Transition Met. Chem. (Weinheim, Ger.) 3 (1978) 253 and refs. cited therein. (b) M.F. Lappert, P.P. Power, A.R. Sanger, R.C. Srivastava, Metal and Metalloid Amides, Ellis Horwood, Chichester, 1980 and ref. cited therein. (c) C.E. Laplaza, C.C. Cummins, Science 268 (1995) 861. (d) C.C. Cummins, R.R. Schrock, W.M. Davis, Organometallics 11 (1992) 1452. (e) Z. Duan, M. Schmidt, V.G. Young, X. Xie, R.E. McCarlet, J.G. Verkade, J. Am. Chem. Soc. 118 (1996). (f) L Scoles, R. Minhas, R. Duchateau, J. Jubb, S. Gambarotta, Organometallics 13 (1994) 4978. (g) H.C. Aspinall, M.R. Tillotson, Inorg. Chem. 35 (1996) 2163. (h) H.C.S. Clark, F.G.N. Cloke, P.B. Hitchcock, J.B. Love, A.P. Wainwright, J. Organomet. Chem. 501 (1995) 333. (i) W.E. Buhro, M.H. Chisholm, K. Folting, J.C. Huffman, J.D. Martin, W.E. Streib, J. Am. Chem. Soc. 114 (1992) 557.

[10] See for example: Y. Wielstra, S. Gambarotta, A. Meetsma, J.L. de Boer, Organometallics 8 (1989) 250.

[11] J. Jubb, S. Hao, S. Gambarotta, Inorg. Chem. 34 (1995) 3563.

[12] Y.J. Kim, M.P. Bernstein, A.S. Galiano-Roth, et al., J. Org. Chem. 56 (1991) 4435.

[13] M.B. Mabbs, D.J. Machin, Magnetism and Transition Metal Complexes, Chapman and Hall, London, 1973.

[14] G. Foese, C.J. Gorter, L.J. Smits, Constantes Selectionnées Diamagnetisme, Paramagnetisme, Relaxation Paramagnetique, Masson, Paris, 1957.

[15] D.T. Cromer, J.T. Waber, International Tables for X-ray Crystallography, Kynoch Press, Birmingham, UK, 1974.